Applied Thermal Engineering 230 (2023) 120725

Contents lists available at ScienceDirect

Applied Thermal Engineering

journal homepage: www.elsevier.com/locate/apthermeng

Research Paper

# Testing of Variable-Speed Scroll Compressors and their inverters for the evaluation of compact energy consumption models

Rubén Ossorio *, Emilio Navarro-Peris

*Instituto Universitario de Investigación en Ingeniería Energética (IUIIE), Universitat Politècnica de València, Camino de Vera s/n, ed. 8E cubo F 5°, 46022 Valencia, Spain*

ARTICLE INFO

*Keywords:*
Variable speed compressor
Inverter
Efficiency
Modelling
Consumption

ABSTRACT

Prediction models for energy consumption in heat pumps are critical for design, selection, control and fault detection. However, nowadays, the methodology for characterizing variable-speed compressors has not been standardized, and typically the pair compressor-inverter is studied as a whole. In this study, disaggregated energy consumption results of compressor and inverter are provided by using a double-wattmeter scheme. These results are used to compare the performance of existing models and to establish guidelines to define testsmatrixes as compact as possible to characterize this type of compressors. The widely used 20-coefficient correlation can overfit the compressor behaviour when fitted with an small dataset, introducing significant deviations when extrapolating. Optimal Design methodologies to create rating test matrixes gave excellent results compared with classical clustering techniques. Regarding inverter results, a compact empirical model was proposed to model inverter power losses depending on total consumption and compressor speed. The proposed model used only five fitting coefficients, and most predictions are inside a 5% error band for all tested inverters. Finally, the tested compressors and inverters suffered a significant efficiency loss at very low speeds, which could make cycling more profitable under certain circumstances.

## 1. Introduction

Heat pump systems have spread into the heating and air conditioning industry as they offer an efficient, affordable, and reliable solution. The EU considers them the path to follow in heating and cooling to reach the objectives of reducing CO2 emissions.

As thermal loads tend to be highly variable, heat pumps have to work at part load for most of their lifetime. Consequently, capacity control techniques have to be applied, among which the use of variable speed compressors (VSC) stands out [25,12]. This technology enhances energy savings compared with On/Off systems using single-speed compressors [5,26], which have been gradually replaced by variable speed solutions since Toshiba introduced the technology into the HVAC sector in 1981 [34].

The compressor is the heart of a heat pump and its most complex element. Consequently, a compressor simulation model that provides information about consumption is essential in designing or studying an HVAC system. In the literature, three different approaches are typically found when modelling a single-speed compressor [31]:

- **Detailed**. [11,7] They consider internal geometries, leakages, oil properties and heat dynamics inside the compressor. They require many parameters based on information that only manufacturers have and are computationally intensive. They provide accurate results but are used mainly for compressor design.
- **Efficiency-based** (Also called semi-empirical). [9,17,33,22,18]. These models are derived from the physical work equation of vapour compression and use experimental data to deduce parameters that are hard to determine as polytropic coefficients, losses to the ambient and heat transfer coefficients, among others. These are models with a low number of fitting parameters. However, they may be difficult to adjust as they involve non-linear equations, typically with exponents, and their accuracy is limited.
- **Map-based** (or Empirical) [2,28,6] They don't require any physical information about the internal processes of the compressor. They typically consist of polynomial equations whose coefficients are fitted with experimental data.

The problem with map-based models is overfitting. A model with many coefficients will constantly adjust the training dataset better; however, it may result in fitting non-useful information as experimental

* Corresponding author.
*E-mail address:* r.ossorio@iie.upv.es (R. Ossorio).

https://doi.org/10.1016/j.applthermaleng.2023.120725
Received 29 December 2022; Received in revised form 3 May 2023; Accepted 3 May 2023
Available online 14 May 2023

**Nomenclature**

*Abbreviations*

| | |
|---|---|
| CV | coefficient of variance of RMSE |
| MRE | maximum relative error |
| POE | polyolester oil |
| PDOE | Polygon Design of Experiments |
| PR | Pressure Ratio |
| PVE | polyvinyl ether oil |
| OD | optimal design |
| RMSE | root mean square error |
| SC | subcooling |
| SH | superheat |

*Symbols*

| | |
|---|---|
| $f$ | compressor speed [Hz] |
| $k_{\#}$,$s_{\#}$,$c_{\#}$ | fitting coefficients |
| $\dot{m}$ | mass flow [g/s] |
| MW | molecular weight [g/mol] |
| $P$ | pressure [bar] |
| $R$ | 8.314 [J/(K·mol)] |
| $T$ | temperature [K] |
| V | compressor displacement [$m^3$] |
| $\dot{W}$ | electrical power [W] |

*Subindex*

| | |
|---|---|
| amb | ambient |
| c | condensing |
| compr | compressor |
| d | discharge |
| e | evaporating |
| in | input |
| inv | inverter |
| is | isentropic |
| nom | nominal |
| out | output |
| ref | at nominal speed |
| s,suc | suction |
| v | volumetric |

*Greek letters*

| | |
|---|---|
| η | efficiency |
| κ | isentropic exponent [-] |
| $\rho$ | density [$kg/m^3$] |

error. When this happens, the model will fail to perform accurately against unseen data [15]. To avoid underfitting or overfitting, the model needs to have a suitable complexity in agreement with the level of information embedded in the train data. Choosing between model accuracy and model complexity is critical for map-based model development.

When modelling a **fixed-speed compressor**, the most extended methodology is the AHRI correlation which uses ten coefficients [29,2] (represented in Eq.(1)). It is a map-based model that uses evaporating and condensing temperatures as modelling variables and can be used to predict compressor consumption and refrigerant mass flow, among others.

$$\dot{W}_{compr} = k_1 + k_2 T_e + k_3 T_c + k_4 * T_e^2 + k_5 T_e T_c + k_6 T_c^2 + k_7 T_e^3 + k_8 T_e^2 T_c + k_9 T_e T_c^2 + k_{10} T_c^3 \quad (1)$$

According to Aute et al. [4], manufacturers typically take more than 14 experimental points to fit the correlation and test 2–3 different units for accounting for unit-to-unit variations.

However, there is no general characterization procedure when talking about variable-speed compressors. Typically, VSC are studied as a family of fixed-speed compressors, and the performance of the VSC is provided with an AHRI 10 coefficient correlation for each different speed. In its selector software, Bitzer uses this methodology [35], and it appears in some publications [24]. This methodology would imply interpolations between speeds and testing 14 different compression conditions at each speed which is cumbersome and time-consuming.

Nowadays, the state of art of VSC modelling is to use an expanded version of the widely known 10-coefficient AHRI correlation [2]. The new function introduces ten additional speed-dependent coefficients resulting in a 20-coefficient correlation which will be called from now on AHRI-20 (displayed in Eq.2).

$$\begin{aligned}\dot{W}_{compr} = {} & k_1 + k_2 T_e + k_3 T_c + k_4 f + k_5 T_e^2 + k_6 T_c^2 + k_7 f^2 + k_8 T_e T_c + k_9 T_e f \\ & + k_{10} T_c f + k_{11} T_e^3 + k_{12} T_c^3 + k_{13} f^3 + k_{14} T_e^2 T_c + k_{15} T_e^2 f + k_{16} T_c^2 T_e \\ & + k_{17} T_c^2 f + k_{18} f^2 T_e + k_{19} f^2 T_c + k_{20} T_e T_c f\end{aligned} \quad (2)$$

This polynomial expression is used by manufacturers such as Emerson or Danfoss in their catalogue data [36,37] and has been used in the literature for modelling variable-speed heat pumps [13,30]. It tends to adjust well train data due to the high number of fitting coefficients. However, many tests are required to fit the model correctly, and the extrapolation capabilities are limited.

Apart from AHRI-20, other variable-speed models have been published [28,19,27,21], which are reviewed in a following section. To compare the performance of the different correlations, real experimental data is needed and, for this matter, data in the compressor datasheets can't be used as it typically consists of predictions from a pre-adjusted model, not the actual test results. Consequently, that data can not be used to perform a fair comparison among models as it will perfectly fit the model from which it was generated.

In the literature, there are few experimental datasets of variable-speed compressor performance. Shao et al. [28] presented performance data of a rotary compressor. However, the study did not provide individual results but the fitted correlations instead and did not declare the number of training points and where they were positioned. In Darr and Crawford's study [10], individual experimental results are given for different temperatures and speeds for an automotive reciprocating compressor. However, the data was not evenly distributed, and only a local portion of the envelope was tested. Consequently, significant extrapolations are needed to model the complete envelope. Cuevas and Lebrun [8] also provided experimental data (50 different compression conditions distributed at five different speeds) for a variable-speed scroll compressor working with R134a.

In addition to introducing a new variable in the compressor

modelling (the speed), using variable-speed compressors introduces another component, the inverter or Variable Frequency Drive (VFD). This element also generates losses which are challenging to characterize due to the difficulty of measuring electrical power at the inverter outlet. As a consequence, the pair compressor-inverter is typically considered a black box, and only the global consumption is measured.

The inverter performance has been studied thoroughly in the electrical field, where good prediction models can be obtained using as input variables: output currents, DC bus voltages, technology of the switching devices, control algorithms… However, this information is rarely available in the HVAC field, and correlations based on easy-to-obtain variables such as consumption or speed would be of particular interest.

According to Afjey and Jenni [1], two separate losses are introduced when using an inverter. The firsts are primary losses which are produced in the inverter itself. They include conduction, commutation and base power losses. Secondary losses are generated in the compressor and are related to the PWM signal's harmonics created by the inverter. The latter are often neglected when the switching frequency exceeds 1 kHz [1].

Cuevas and Lebrun [8] studied the inverter power losses through a calorimetric method. They concluded that the inverter efficiency depended mainly on the output power, not the speed. The reported losses were in the range of 2–5% and a correlation to model power losses was not proposed.

In this study, a complete experimental characterization of variable-speed systems is made. This study is split into two parts; the first focuses on heat pump compressors and the second on inverter performance.

The first part starts analyzing the compressor's experimental results. Then, the experimental data is used to review the performance of already published compressor models. And finally, the problem of how to select the rating points is assessed.

The second part focuses on inverter power losses. A novel mathematical model is proposed to predict the power losses of the tested inverters, and the carrier frequency influence is evaluated.

## 2. Methodology

### 2.1. Test bench description

The compressor test bench described in Fig. 1 has been used to characterize variable-speed compressors. It has been designed to satisfy the Standard EN13771 [38] for compressor rating and can evaluate the typical compression cycle conditions varying condensing and evaporating pressure, subcooling (SC), superheat (SH) and compressor speed. The test bench comprises a set of PID controllers that can keep any operating condition stable within a range of 1 kPa and 0.1 °C from its reference without manual adjustments.

The installed sensors are described in Table 1 and their uncertainty is displayed at a confidence interval of 95%. The temperature readings were taken by immersion RTDs placed in an elbow facing upstream. Methods A and E of the Standard EN13771 [38] were implemented to measure mass flow: a Coriolis sensor placed in the refrigerant liquid line and a calorimetric balance in the evaporator. Regarding energy consumption, a double-wattmeter scheme was used to determine power losses in the inverter and the global consumption. A YOKOGAWA WT1030 [14] power meter was implemented in the line connecting the inverter and the compressor, as it is capable of measuring electrical power in this line. This line cannot be measured with typical power meters as it presents a high-frequency square wave voltage in the range of the kHz result of the pulse width modulation (PWM) needed to control the compressor speed [1].

Sensor readings were logged with a Keysight 34970A and the final result was the average of all the measurements taken in a stable window of at least 15 min (typically 30 min). The thermodynamic database used was REFPROP v10.0 [16], which was used to calculate evaporating and condensing temperatures as a function of the corresponding pressures.

### 2.2. Experimental data

In this test bench, two variable-speed scroll compressors from diverse manufacturers and working with different refrigerants were tested: Compressor A and Compressor B. Both presented the same typology; the compression chamber at the top position (above the electric motor) and the lubrication mechanism consisting of a borehole in the shaft that acts as a pump to lubricate the main bearings and the scroll.

Compressor A has a displacement of 46 $cm^3$ and works with R290 and POE68 oil. It has been tested at distributed conditions of evaporating and condensing temperatures, trying to map the entire envelope homogeneously. To correctly map the entire speed range (15–120 Hz), that pattern was repeated at speeds of 30, 50, 70, 90 and 110 Hz resulting in a total of 134 experimental tests. The tested conditions for each speed are represented in Fig. 2.

Compressor B is a variable-speed scroll compressor with a displacement of 44.5 $cm^3$ and works with R410A and PVE32 as a lubricant. In total, 35 different compression conditions were tested, 14 at the nominal speed of 60 Hz, and the rest distributed along the envelope at different

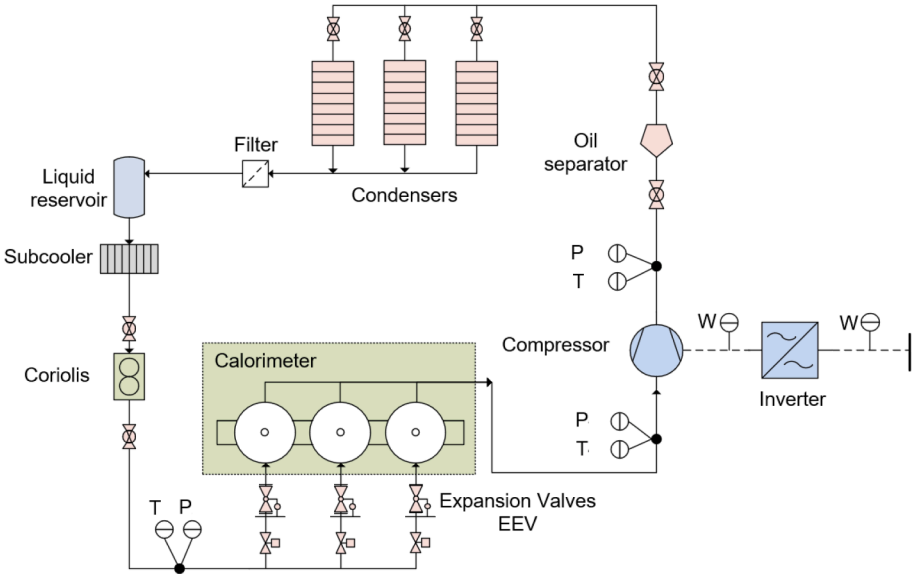


**Fig. 1.** Variable-Speed Compressor Test Bench.

**Table 1**
Sensors used and their uncertainty.

| Uncertainty of the used sensors | | |
|---|---|---|
| Variable | Equipment | Uncertainty |
| T | RTD-PT | ±0,05 °C |
| P | Fisher-Rosemount 3051 | ±0,02% |
| $\dot{m}$ | Coriolis CMF025M | ±0,025gs-1 |
| Win | Fluke 1735 | ±51 W |
| Wout | Yokogawa WT1030 | ±13 W |

frequencies.

Additionally, the experimental data obtained by Cuevas and Lebrun [8] was also included so the models are evaluated against three different compressor models with three different refrigerants.

In Table 2, a summary of the used datasets is displayed.

Apart from the tested compressors, the mentioned test bench was also used to characterize three different inverters from different manufacturers. All of them used the same control strategy (Advanced Open Loop Control for Permanent Magnet Motors) to adjust the compressor speed with carrier frequencies ranging from 6.6 kHz to 5 kHz. As the electrical motors are synchronous, the slip ratio has not been considered, and the mechanical speed of the compressor has been supposed to be the same as the one configured in the inverter. A summary of the specifications of each tested inverter is displayed in Table 3.

## 3. Compressor performance

### 3.1. Analysis of the experimental results

The detailed experimental results of compressors A and B are included as complementary materials and in this section, the experimental data of Compressor A will be studied in detail as it is the one with more tested conditions.

The experimental mass flow results are displayed in Fig. 3. It should be noted that the main variables affecting the mass flow are evaporating temperature and speed.

In Fig. 4, the experimental results of the compressor consumption (including inverter losses) are displayed at different compression conditions. The peak consumption was close to 7 kW and was produced at maximum speed and PR.

Compressor efficiency is defined in Eq.(3), and its evolution with the compression conditions can be seen in Fig. 5.

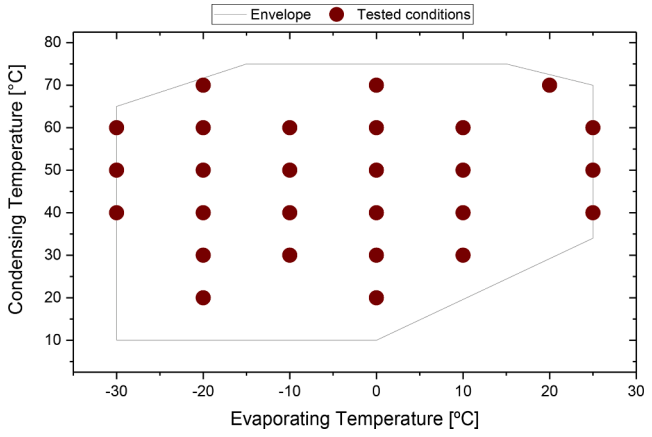


**Fig. 2.** Test Matrix of Compressor A.

**Table 2**
Summary of the experimental data set used for the evaluation of the consumption models.

| | Compressor A | Compressor B | Compressor C |
|---|---|---|---|
| Source | Experimental | Experimental | Cuevas [8] |
| Technology | Scroll | Scroll | Scroll |
| Displacement | 46 $cm^3$ | 44.5 $cm^3$ | 54.25 $cm^3$ |
| Refrigerant | R290 | R410A | R134a |
| Lubricant | POE 68 | PVE 32 | – |
| Speed Range | 15–110 Hz | 15–100 Hz | 35–75 Hz |
| Nominal Speed | 70 | 60 | 50 |
| SH | 10 K | 10 K | 4–9 K |
| Tests | 134 | 35 | 48 |

$$\eta_{compr} = \frac{\dot{m}\left(h_{d,is} - h_s\right)}{W_{compr}} \tag{3}$$

It should be pointed out that compressor efficiencies behave homogeneously, showing a maximum at PR close to 2.5 and sharply decreasing as PR decreases or increases. At central speeds (50, 70 and 90 Hz), compressor efficiency doesn't show a significant dependence on speed. However, a decrease in compressor efficiency is manifested at low frequencies and high condensing temperatures. The main explanation for this phenomenon is a lack of lubrication in the scrolls at low speeds, which increases frictional losses and internal leakages. The internal leakages are related to the pressure difference, which explains why these become more relevant at high condensing temperatures. The hypothesis of low lubrication at low speeds was analyzed in a previous study [23] and was also pointed out by Cuevas and Lebrun [8].

Compressor efficiency also decreases at high speeds and low condensing temperatures due to an increase in mechanical losses. These mechanical losses do not depend heavily on working temperatures; consequently, at lower condensing temperatures where the compressor has a lower consumption, they have a higher impact on efficiency.

### 3.2. Characterization models

This section compares the performance of the main proposed models in the literature for variable-speed compressors. A summary list of the tested correlations is presented in Table 4.

AHRI-20 and Shao are linear empirical correlations that can be easily fitted with ordinary regression tools. However, Santos, W. Li and Mendoza consider fitting exponents whose convergence is more problematic and need more complex regression tools. Santos model is coupled with the mass flow model, and thus, if the mass flow measurements have a significant experimental uncertainty, it will also propagate to the consumption estimation. In this study, to minimize this effect, the values of mass flow introduced in the consumption model will be the ones predicted by the pre-adjusted mass flow model. That way, the experimental uncertainty of mass flow is partially filtered and will lower the consumption estimation error.

All these correlations were fitted using the complete dataset, and the fitting results are displayed in Fig. 6. For the comparison, the Coefficient of Variation (CV) of the Root Mean Square Error (RMSE) was used (Eq.

**Table 3**
Summary of the experimental data set used for the evaluation of Inverter energy consumption.

| | Inverter A | Inverter B | Inverter C |
|---|---|---|---|
| Tests | 133 | 17 | 35 |
| Carrier Frequency | 6 kHz | 6.6 kHz | 5 kHz |
| Tested Power | 0.7–7 kW | 0.7–5 kW | 0.6–7 kW |
| Max Power | 15 kW | 5.5 kW | 10 kW |
| Tested Speed | 15–110 Hz | 15–110 rpm | 15–100 rpm |
| Efficiency | 0.87–0.96 | 0.91–0.94 | 0.90–0.98 |
| Control mechanism | Open Loop Control for Permanent Magnet Motors | | |

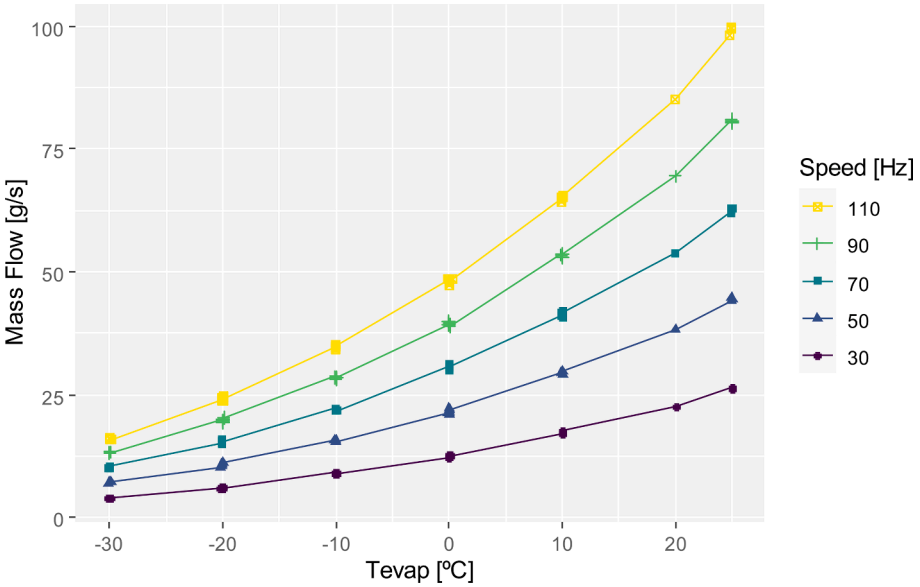


**Fig. 3.** Experimental Mass Flow evolution with compression condition and speed [Compressor A].

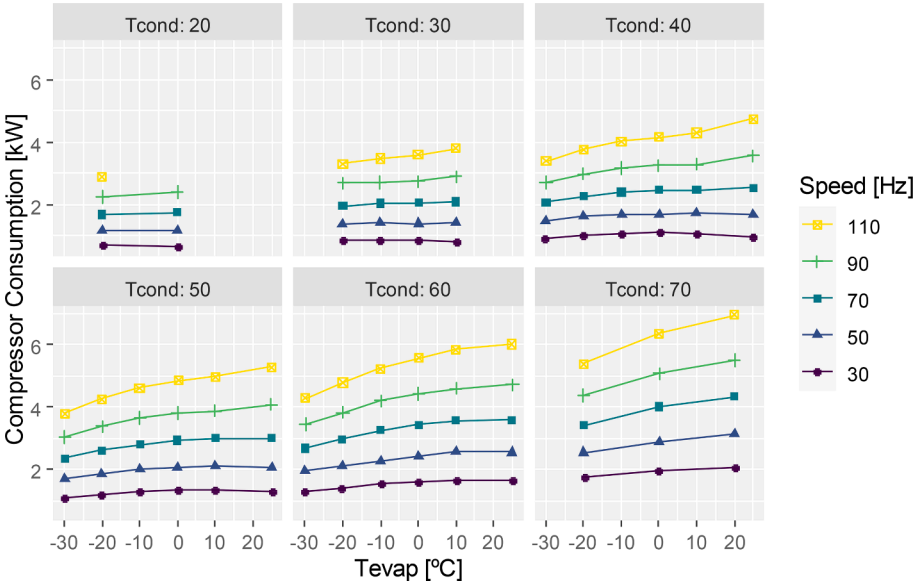


**Fig. 4.** Consumption evolution with the compression condition and speed [Compressor A].

(4)), an adimensional parameter that measures the relative dispersion of the error in the modelled variable. As the RMSE is divided by the tested consumption mean, the results from the different compressors can be compared even if their sizes are not the same. RMSE (in W) is also shown in the plot to compare it with the sensor accuracy (in the range of 50 W).

$$CV(RMSE) = \frac{RMSE}{\overline{X}} = \frac{1}{\overline{X}}\sqrt{\frac{\sum_{n=1}^{N}(\hat{y}_t - y_t)^2}{N}} \tag{4}$$

The correlation with better performance is AHRI-20 with RMSE values lower than 50 W in all the studied compressors. It is followed by Shao correlation, and then, the other correlations change order depending on the tested compressor. In general, the one having higher errors is Santos. However, it should be noted that it is also the correlation with fewer coefficients (only 3).

Remark that the results were obtained using all available data and models containing more variables will always perform better when the dataset is extensive. However, when the train data decreases, they can overfit it and fail to predict new data correctly. Train-test fitting can be performed to check for overfitting, which consists of adjusting the correlations with a limited dataset (train) and then calculating the goodness of predictions for the complete dataset (test). If the correlation is overfitted, it will try to model the experimental noise in the train set, giving poor predictions with the entire data.

### 3.3. Design of experiments

According to Aute et al. [4], manufacturers typically take 14–20 conditions when characterizing a fix-speed compressor. However, to fit the AHRI-20 correlation, at least 20 tests are needed, 21 if statistics to measure the goodness of fit are required (RMSE, MRE, CV…). Fig. 7 shows the result of the train-test procedure repeated 100 times. In the first plot, the 21 train tests were selected randomly. In the second one, the selection was made by distributing the training samples homogeneously along the envelope with a clustering technique. It should be noted that the same 100 train sets were applied to the different

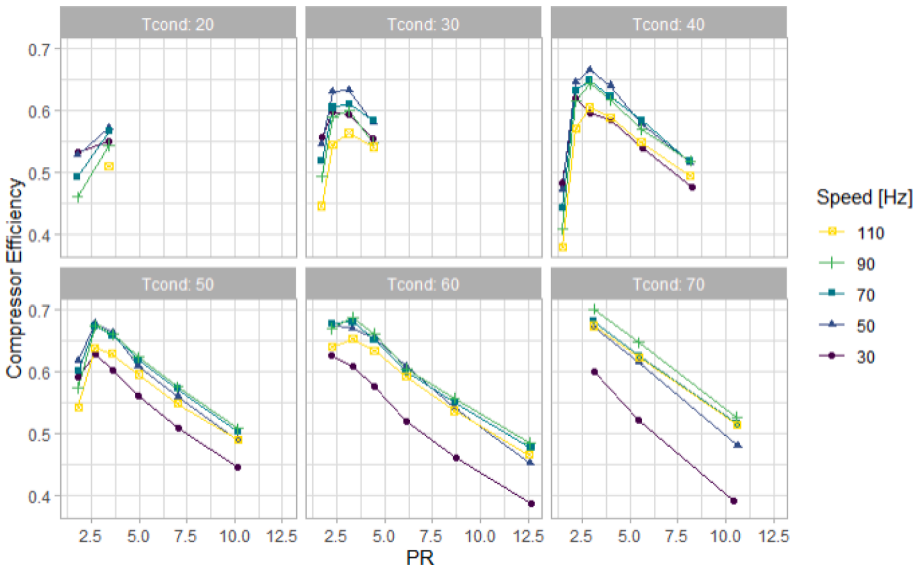


**Fig. 5.** Compressor A efficiency and its evolution with the working variables.

**Table 4**
List of models fitted with the experimental data.

| ID | Expression | Coef | Var |
|---|---|---|---|
| AHRI-20 [13] | $\dot{W}_{compr} = k_1 + k_2T_e + k_3T_c + k_4f + k_5T_e^2 + k_6T_c^2 + k_7f^2 + k_8T_eT_c + k_9T_ef + k_{10}T_cf + k_{11}T_e^3 + k_{12}T_c^3 + k_{13}f^3 + k_{14}T_e^2T_c + k_{15}T_e^2f + k_{16}T_c^2T_e + k_{17}T_c^2f + k_{18}f^2T_e + k_{19}f^2T_c + k_{20}T_eT_cf$ | 20 | 3 |
| Mendoza [21] | $\eta_{compr} = \left(\frac{P_d}{P_s}\right)^{k_1}\left(\frac{f_{nom}}{f}\right)^{k_2}\left(\frac{f^3V}{\frac{3}{\Delta h_{iso}^2}}\right)^{k_3}\left(\frac{\Delta h_{iso}\rho_s}{P_s}\right)^{k_4}\left(\frac{T_s}{\left(\frac{T_s+T_{d,is}}{2}\right)-T_{amb}}\right)^{k_5}$ $W_{compr} = \frac{\dot{m}(h_{d,is}-h_s)}{\eta_{compr}}$ | 6 | 8 |
| Santos[27] | $\dot{W}_{compr} = \dot{m}\left[k_1T_s\left[\left(\frac{P_d}{P_s}\right)^{k_2}-1\right]+k_3\right]\dot{m} = \frac{P_sf}{T_s}\left\{b_0+b_1\left[\left(\frac{P_d}{P_s}\right)^{b_2}-1\right]\right\}$ | 3 | 4 |
| Shao [28] | $\dot{W}_{compr} = (k_1+k_2T_e+k_3T_c+k_4T_e^2+k_5T_c^2+k_6T_eT_c)\left[s_0+s_1\Delta f+s_2\Delta f^2\right]$ (rotary) | 9 | 3 |
| W. Li [19] | $\dot{W}_{compr} = \left\{P_sVf_ck_1\left[\left(\frac{P_d}{P_s}\right)^{k_2+\frac{\kappa-1}{\kappa}}+\frac{k_3}{P_d}\right]+k_4\right\}\left[s_0+s_1(f/f_{nom})+s_2(f/f_{nom})^2\right]$ | 6 | 4 |

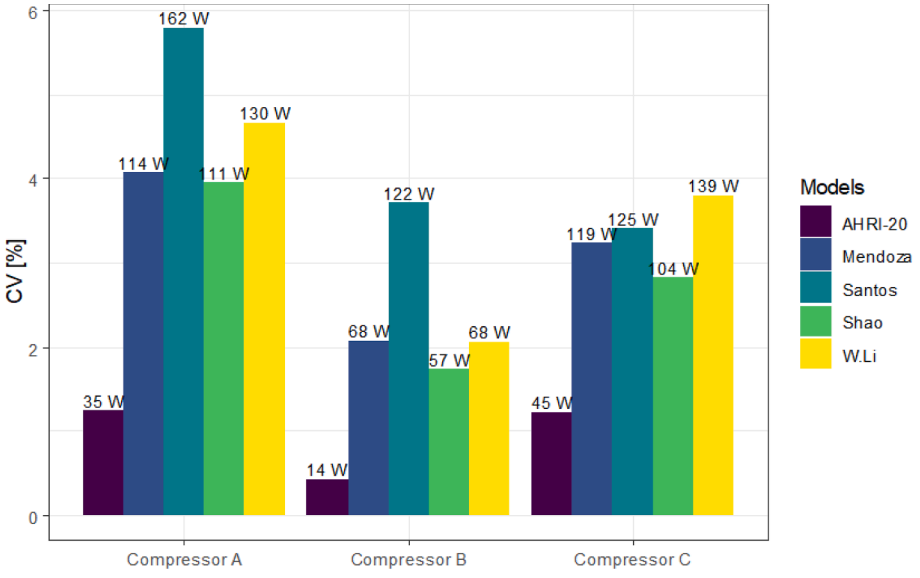


**Fig. 6.** Performance of the different models fitted to various compressor datasets.

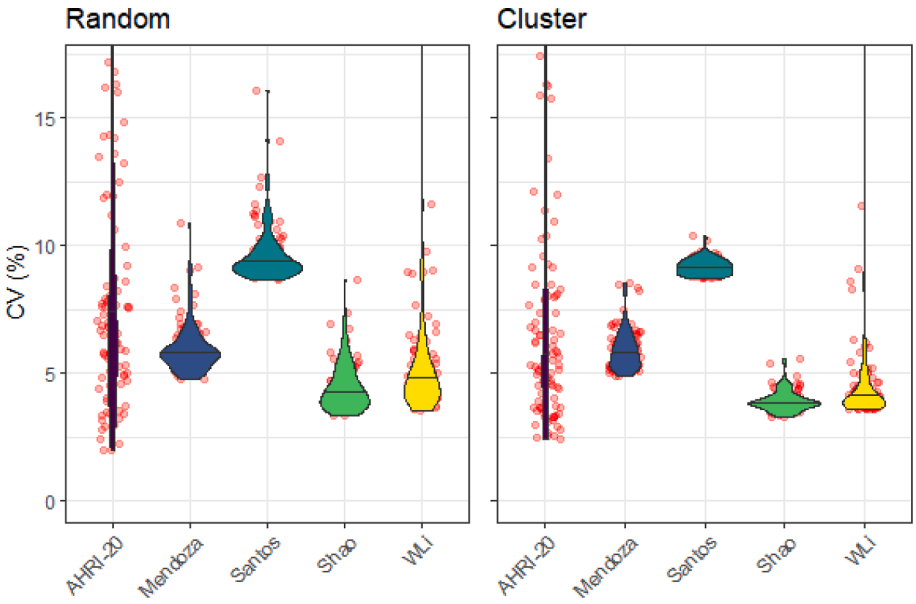


**Fig. 7.** Robustness of the different models when adjusted with 21 tests selected randomly (Left) or with a clustering methodology (right).

correlations, so a poorly chosen trainset would affect all models. The red dots in the plot represent the fitting accuracy of each of the 100 runs and the shapes describe a violin plot representing a vertical density function of the results in which the horizontal line describes the median.

Results show significant variability for AHRI-20, even if the samples are evenly distributed along the envelope. This indicates that this correlation tends to overfit the train data and, a lot of experimental data is required to adjust it correctly, increasing the compressor characterization cost. Regarding the rest of the data, Shao tends to perform best most of the time with limited variability. W. Li follows Shao but presents a higher variability with a couple of points in which the solution did not converge. And finally, the one with a worse average performance is Santos which was expected with only 3 fitting coefficients.

Another conclusion from Fig. 7 is that the results' variability also depends on the strategy followed to select the train data, as selecting distributed points improves the performance. Hence, another way of decreasing the variability would be to choose the position of the train tests wisely.

According to Aute [4] there isn't a well-established methodology among manufacturers to address the positioning of the train data. Aute [4] used a conventional approach called Latin Hypercube Sampling for fixed-speed compressors and presented a new methodology for non-rectangular domains. This new method was called Polygon Design of Experiments (PDOE) which combined the clustering technique with manually picking extreme conditions at the vertices of the envelope. Lately, Marchante [20] suggested the use of Optimal Design (OD) methodologies [3]; these methodologies take as input the model equation, the required number of train test and a list of candidates points and return the train set that minimizes the generalized variance for the fitting coefficients. The calculations involve some intensive statistical calculations, but open-source tools implement the algorithms, resulting in an easy-to-use methodology to obtain optimized train sets. In this study, the function optFederov of the package AlgDesign [32] was used with the D-Optimal criteria [3] for linear models. It should be noted that, when either the candidate and the train set size are big, it does not exist a clear optimum and multiple train sets can be obtained from the algorithm if it is run multiple times.

In this study, the OD methodology was extrapolated to the rating point selection of variable-speed compressors. Fig. 8 shows a train set resulting from applying OD to the model AHRI-20 with a train set size of 21. The optimization algorithm considered extreme points close to the vertexes of the envelope and some at medium speeds, which would reassemble the train points obtained if PDOE method [4] had been used.

If this approach is followed to fit the AHRI-20 model with 21 train conditions, a RMSE of 80 W is obtained when the model is used to predict the entire dataset. This value lies in the lower portion of the results obtained in Fig. 7 using clustering.

In order to apply this methodology to Shao's model, it was divided into two decoupled models as originally presented by his author: one for a nominal speed with 6 coefficients and the other with 3 coefficients to consider the speed effect. The OD methodology was applied for the nominal speed with a desired train size of 7, and then 2 points were added at extreme speeds to adjust the speed effect. Those 2 points at extreme speeds were added in the center of the envelope as those points tend to be easier to test and Shao states that the speed effect does not depend on the compression conditions. The complete test matrix is displayed in Fig. 9, it can be noted how the OD algorithm also selected rating points close to the envelope vertexes and one in the centre.

If Shao's model is fitted with this train set and then it is used to predict the entire dataset, a RMSE of 101 W is obtained, which is remarkable with only 9 train tests. Better fit even compared to using the whole dataset.

The results of this chapter highlight the importance of a good rating matrix design (number of rating points and their location) for compressor characterization. Using the Optimum Design methodology allowed to obtain high precission fits for all the envelope using only 9 rating points. These same 9 rating points could also be used to fit mass flow correlations as its behaviour is smoother and easier to model compared with power consumption [20].

## 4. Inverter performance

### 4.1. Inverter model

This section aims to study how inverter losses depend on the compression condition and speed and then an empirical correlation based on accessible variables such as global consumption and speed is provided. The obtained data for all three tested inverters can be accessed in the complementary materials, but only the inverter A dataset will be shown in this section due to space limitations.

Fig. 10 shows the evolution of efficiency and power losses of the tested Inverter A as a function of speed and total consumption. Inverter

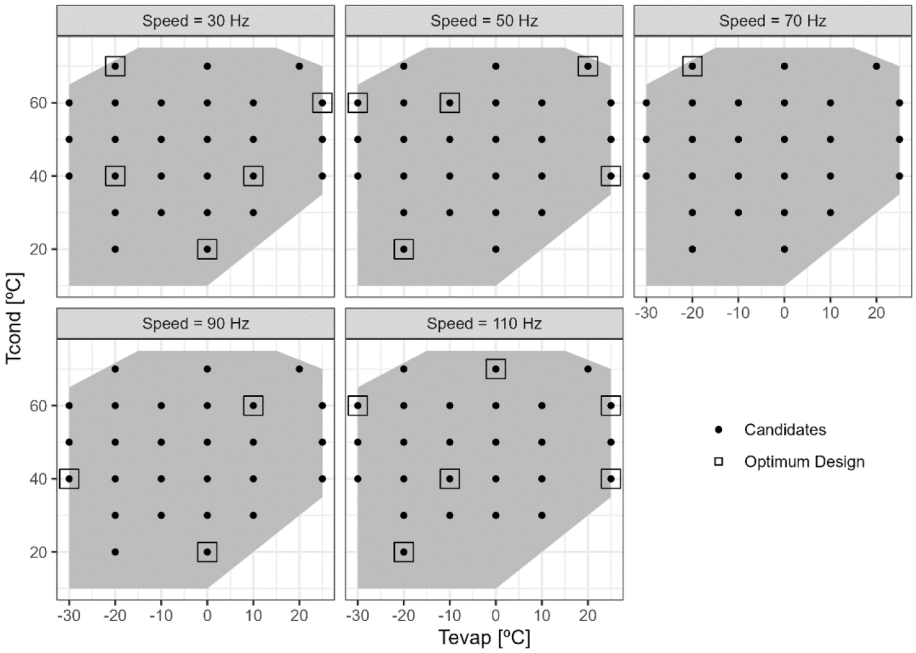


**Fig. 8.** Train set selection using Optimal Design for AHRI-20 model.

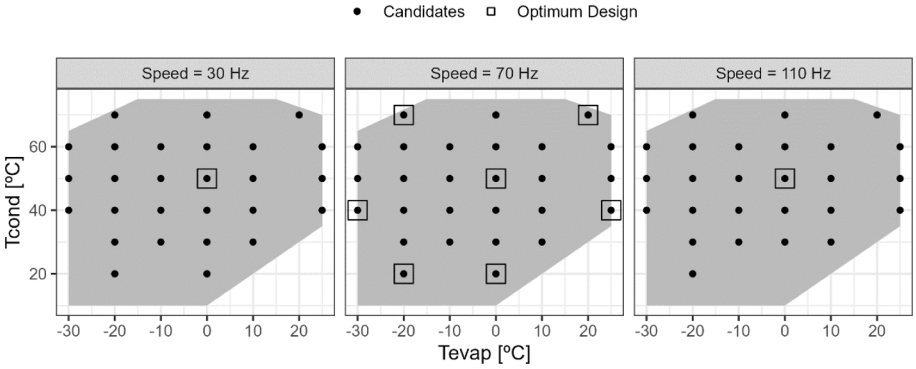


**Fig. 9.** Train set selection using Optimal Design for Shao.

efficiency mainly depends on power consumption; as consumption decreases, efficiency drops to values lower than 90%. In this inverter, the efficiency homogeneously increases as consumption increases, however, in other inverters (p.e. Inverter B), the efficiency finds a maximum, and then the efficiency starts decreasing as consumption keeps rising.

Furthermore, it has been found that speed also impacts efficiency, contrary to what Cuevas and Lebrun [8] found using the calorimetric method. This discrepancy can be explained as Cuevas and Lebrun [8] tested over a limited speed range, and the efficiency variation due to speed fell in the method's uncertainty band.

To model the behaviour of the inverter, it was preferred to model the evolution of power loss instead of efficiency, as it resulted in a more linear tendency with consumption and speed. The resulting model (Eqn 5) has five fitting coefficients and can be adjusted easily with conventional regression tools.

$$\dot{W}_{loss} = c_0 + \left[s_0 + s_1\Delta f + s_2\Delta f^2\right]\dot{W}_{in} + c_2\dot{W}_{in}^2 \tag{5}$$

The proposed model fits reasonably well all VSDs tested. The model performance is displayed in Fig. 11, showing an RMSE of 5 W and around 95% of the experimental results fall in the range of 5% error. The model performance can also be checked in Fig. 10, where the lines represent the predicted values of the proposed model applied to Inverter A.

The fitted parameters of all three tested inverters are listed in Table 5 and its worth noting that the order of magnitude of the different coefficients is similar for the various inverters. The intersect provides information about the device's no-load consumption, which can be accessed directly from the datasheets. Additionally, it has been included the significance level of the different coefficients using the following standard notation (+p < 0.1, * p < 0.05, ** p < 0.01, *** p < 0.001). The significance of C2 can give us information about the general behaviour at high inverter consumption. For low significance (Inverter A), efficiency keeps increasing as consumption increases, but for high significance (Inverter B), inverter efficiency finds a maximum and decreases as consumption further increases. This behaviour also is present in inverter C but only at very high speeds and consumptions.

For Inverter C, the fitting errors are greater because the model, due to its simplicity, didn't fit a particular behaviour correctly at low speeds. Nevertheless, apart from those samples, most predictions entered in the range of 5% error and RMSE was lower than 6 W.

### 4.2. *Effect of the carrier frequency*

Carrier frequency is the rate at which the transistors are switched, which tends to be in the range of kHz. The higher the frequency the smaller number of harmonics produced at the output signal. However, it

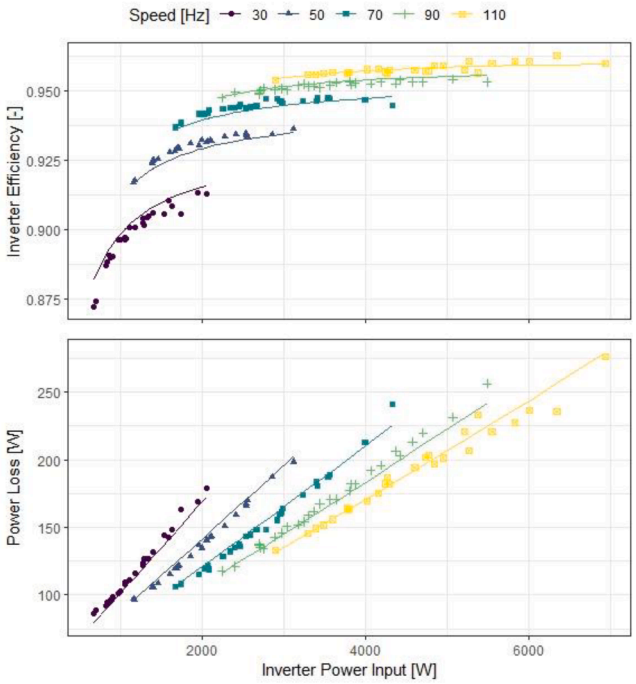


**Fig. 10.** Experimental results and predicted performance of inverter A.

comes at the cost of increasing commutation losses.

To check the effect of the inverter switching frequency on its performance, a parametric study has been carried out with Inverter C. A total of 4 tests at different switching frequencies in the range of 2–10 kHz were carried out at the same compression condition. The results are displayed in Fig. 12.

Driver efficiency clearly decreases as the switching frequency increases. In the studied range, the reduction has been of 1.6 percentual points and it showed quite a linear behaviour. This decrease in efficiency is attributed to higher commutations losses due to the increase in the switching frequency.

Other effect that can be observed in Fig. 12 is a reduction of the power consumed by the compressor ($\dot{W}_{inv,out}$). The compressor works at the same load and speed in all tests; consequently, its consumption should remain constant. Consequently, the decrease in consumption could be explained with a reduction of secondary losses generated in the compressor windings due to harmonics in the electrical power signal, which are reduced as switching frequency increases.

Consequently, as the carrier frequency increases, two opposite effects appear: an increase in power losses in the inverter due to the rise of commutation losses and a reduction in the compressor's secondary losses due to fewer harmonics. The total power at the input of the inverter ($\dot{W}_{inv,in}$ in Fig. 12) takes into account both contributions and seems to have an optimum between 2 and 5 kHz for this inverter. For higher switching frequencies, the increase of commutation losses predominates and the total consumption increases.

The effect of the switching frequency has not been considered in the inverter model as it is not a variable which tends to be modified under regular operation and its impact in total consumption is secondary.

## 5. Conclusion

A complete energy consumption analysis has been made for variable-speed compressors studying the inverter and the compressor independently (not as an aggregated black box). Experimental results of three variable-speed scroll compressors working with three different refrigerants were used to test the performance of multiple published correlations, which raised the following conclusions:

- With a high train set, AHRI-20 correlation gave the best accuracy with errors in the power meter's uncertainty range. However, it tended to overfit the train data when it was trained with a limited number of rating points.
- A correlation with the shape of the one proposed by Shao for rotary compressors, with less than half the coefficients compared with AHRI-20, showed a decent performance with fewer overfitting problems.
- W. Li and Mendoza closely followed Shao's performance with even fewer fitting coefficients, but, on the contrary, they involved non-linear correlations that are harder to adjust.
- Correlation selection is a trade between complexity and accuracy; thus, the optimum model could differ for each application.

Another critical issue studied was which is the minimum number of rating points and where to place them inside the compressor's envelope; the found conclusions are:

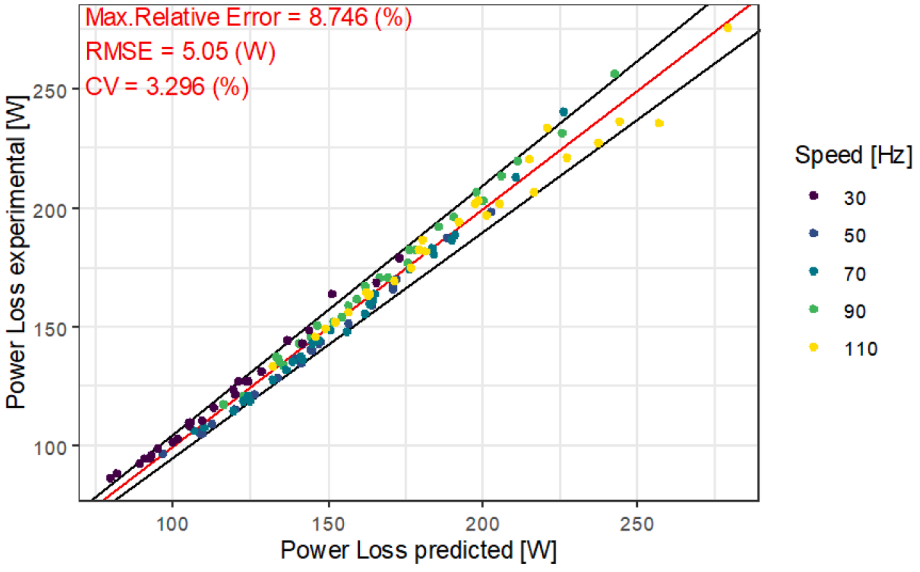


**Fig. 11.** Performance of the inverter model applied to Inverter A.

**Table 5**
Model summary for the tested inverters.

| | INVERTER A | INVERTER B | INVERTER C |
|---|---|---|---|
| **C0** | 3.47E + 01*** | 2.02E + 01*** | 3.27E + 01*** |
| **S0** | 5.25E-02*** | 5.53E-02*** | 1.23E-02** |
| **S1** | −3.01E-02*** | −2.02E-02*** | −1.51E-02*** |
| **S2** | 1.11E-02*** | 3.99E-03*** | 1.72E-03 |
| **C2** | 4.20E-07+ | 4.79E-06*** | 1.71E-06** |
| **NUM.OBS.** | 133 | 17 | 35 |
| **RMSE** | 5.05 | 1.76 | 5.91 |
| **MRE** | 8.75 | 5.26 | 25.55 |
| **CV** | 3.3 | 0.91 | 6.82 |

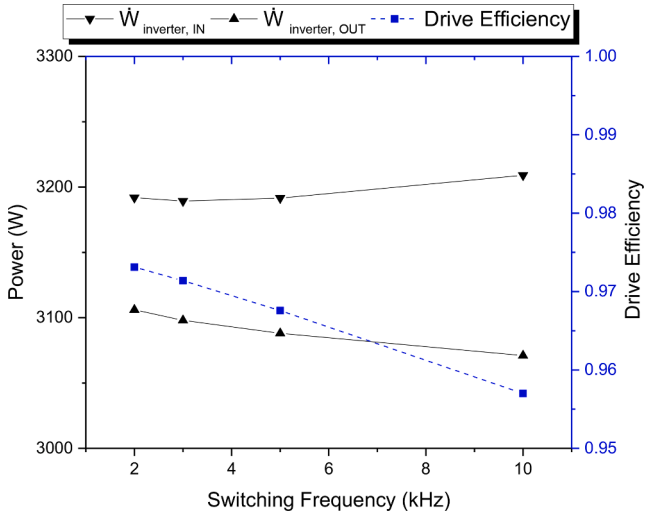


**Fig. 12.** Evolution of Drive Efficiency and Inverter Power Flows with Switching Frequency.

- The Optimal Design methodology permitted the selection of rating points to adjust the correlations with the minimum amount of experimental information.
- With only 9 rating points, predicting the global compressor behaviour with decent accuracy was possible using Optimal Design and Shao's shape correlation.

To study the power losses in the inverter three different devices were tested and the conclusions from the data analysis are:

- The double-wattmeter methodology allowed to detect that power losses depend on either consumption and speed independently.
- A linear five-coefficient correlation is proposed to predict power losses based on variables easy to measure as total consumption or compressor frequency and with typical errors in the band of 5%.
- The switching frequency effect in the complete system is low and was not included in the inverter model as it typically is a predefined parameter that is not changed during regular operation.
- In all tested inverters, the efficiency plummeted at low speeds and total consumption reached losses in the range of 10% (far from the typical 3% constant power loss that is typically considered in the literature). If the compressor efficiency drop at low speeds is also considered, the total penalty of running the compressor at very low frequencies could be so high that other control technics as cycling could be more profitable under certain circumstances.

These findings were obtained from a finite amount of 3 different models. Nevertheless, a previous study [20] stated that scroll compressors behave relatively homogeneously, so the given conclusions are expected to be confirmed with future data. Additionally, as a future work, the strengths and weaknesses of the reviewed models will be analyzed to propose new improved models for consumption, mass flow and discharge temperature.

## Declaration of Competing Interest

The authors declare that they have no known competing financial interests or personal relationships that could have appeared to influence the work reported in this paper.

## Data availability

Data available as complementary materials

## Acknowledgements

The authors would like to acknowledge the Spanish "MINISTERIO DE ECONOMIA Y COMPETITIVIDAD", through the project ref-ENE2017-83665-C2-1-P "Maximización de la eficiencia y minimización del impacto ambiental de bombas de calor para la descarbonización de la calefacción/acs en los edificios de consumo casi nulo" for the given support. In addition, Ruben Ossorio would like to thank the Spanish government for his PhD scholarship with reference PRE2018-083535.

## Appendix A. Supplementary data

Supplementary data to this article can be found online at https://doi.org/10.1016/j.applthermaleng.2023.120725.

## References

[1] T. Afjei, F. Jenni, The Impact of Inverter Losses on, Heat Pump Performance (1994).
[2] Ahri_540. *Ahri Standard 540: Performance rating of positive displacement refrigerant compressors*, 2020.
[3] Anthony C. Atkinson, *Optimal Design. Wiley StatsRef: Statistics Reference Online*, 2015, pp. 1–17. Doi: 10.1002/9781118445112.stat04090.pub2.
[4] Vikrant Aute, Cara Martin, Reinhard Radermacher, AHRI Project 8013: A Study of Methods to Represent Compressor Performance Data over an Operating Envelope Based on a Finite Set of Test Data, Air-Conditioning, Heating, Refrigeration Institute (2015).
[5] G. Bagarella, R. Lazzarin, M. Noro, Sizing strategy of on-off and modulating heat pump systems based on annual energy analysis, Int. J. Refrig. 65 (2016) 183–193, https://doi.org/10.1016/j.ijrefrig.2016.02.015.
[6] C. Aprea, C. Renno, Experimental model of a variable capacity compressor, Int. J. Energy Res. (2008), https://doi.org/10.1002/er.
[7] Yu Chen, Nils P. Halm, James E. Braun, Eckhard A. Groll, Mathematical modeling of scroll compressors, Int. J. Refrig 25 (6) (2002) 751–764.
[8] C. Cuevas, J. Lebrun, Testing and modelling of a variable speed scroll compressor, Appl. Therm. Eng. 29 (2–3) (2009) 469–478, https://doi.org/10.1016/j.applthermaleng.2008.03.016. Oil details in the paper tooScroll variable speed OCR calculations.
[9] Cristian Cuevas Jean Lebrun Vincent Lemort. Eric Winandy Characterization of a scroll compressor under extended operating conditions. Applied Thermal Engineering [online]. 1 May 2010. Vol. 30, no. 6–7, p. 605–615. [Accessed 5 February 2019]. Doi 10.1016/J.APPLTHERMALENG.2009.11.005. Available from: https://www.sciencedirect.com/science/article/pii/S1359431109003330.
[10] J.H. Darr, R.R. Crawford, Conditioning, Air. Modeling of an Automotive Air Conditioning Compressor Based on Experimental Data Acustar Division of Chrysler Bergstrom Manufacturing Co . Ford Motor Company General Electric Company Harrison Division of GM ICI Americas , Inc . Modine Manufacturing Co. P., 1992, vol. 61801, no. February.
[11] M.E. Duprez, E. Dumont, M. Frère, Modelling of reciprocating and scroll compressors, Int. J. Refrig 30 (5) (2007) 873–886, https://doi.org/10.1016/j.ijrefrig.2006.11.014.
[12] E. Granryd, B. Palm, Refrigerating engineering. Stockholm (Sweden) : Royal Institute of Technology, KTH, 2003.
[13] Yabin Guo, Guannan Li, Huanxin Chen, Yunpeng Hu, Limei Shen, Haorong Li, Min Hu, Jiong Li, Développement d'un capteur de puissance de compresseur virtuel à vitesse variable pour un système de conditionnement d'air à débit de frigorigène variable, Int. J. Refrig. 74 (2017) 71–83, https://doi.org/10.1016/j.ijrefrig.2016.09.025.
[14] I. Hisashi, T. Hirotaka, T. Katsuya, H. Kazuo, Models WT1010/WT1030/WT1030M Digital power meters [online], 1997. [Accessed 16 January 2019]. Available from: https://web-material3.yokogawa.com/rd-tr-r00023-003.pdf?_ga=2.86363484.578018800.1547568355-1261763059.1547568355.
[15] Maomao Hu, Fu Xiao, Howard Cheung, Identification of simplified energy performance models of variable-speed air conditioners using likelihood ratio test

method, Sci. Technol. Built Environ. 26 (1) (2020) 75–88, https://doi.org/10.1080/23744731.2019.1665446.
[16] Marcia L. Huber, Eric W. Lemmon, Ian H. Bell, Mark O. Mclinden, The NIST REFPROP Database for Highly Accurate Properties of Industrially Important Fluids, Ind. Eng. Chem. Res. (2022), https://doi.org/10.1021/ACS.IECR.2C01427.
[17] Dagmar I. Jahnig, Douglas T. Reindl, Sanford A. Klein, Semi-empirical method for representing domestic refrigerator/freezer compressor calorimeter test data, ASHRAE Trans. 106 (February) (2000) 2017.
[18] R.N.N. Koury, L. Machado, K.A.R. Ismail, Numerical simulation of a variable speed refrigeration system, Int. J. Refrig 24 (2) (2001) 192–200, https://doi.org/10.1016/S0140-7007(00)00014-1.
[19] Wenhua Li, Simplified steady-state modeling for variable speed compressor, Appl. Therm. Eng. (2013) 318–326.
[20] Javier Marchante-Avellaneda, Jose M. Corberan, Emilio Navarro-Peris, Som S. Shrestha, A critical analysis of the AHRI polynomials for scroll compressor characterization, Appl. Therm. Eng. Vol. 219, no. PA (2023), https://doi.org/10.1016/j.applthermaleng.2022.119432.
[21] J.M. Mendoza-Miranda, A. Mota-Babiloni, J.J. Ramírez-Minguela, V.D. Muñoz-Carpio, M. Carrera-Rodríguez, J. Navarro-Esbrí, C. Salazar-Hernández, Comparative evaluation of R1234yf, R1234ze(E) and R450A as alternatives to R134a in a variable speed reciprocating compressor, Energy 114 (2016) 753–766, https://doi.org/10.1016/j.energy.2016.08.050.
[22] E. Navarro, E. Granryd, J.F. Urchueguía, J.M. Corberán, A phenomenological model for analyzing reciprocating compressors, Int. J. Refrig 30 (7) (2007) 1254–1265, https://doi.org/10.1016/j.ijrefrig.2007.02.006.
[23] Rubén Ossorio, Emilio Navarro-Peris, Study of oil circulation rate in variable speed scroll compressor working with propane, Int. J. Refrig 123 (2021) 63–71, https://doi.org/10.1016/j.ijrefrig.2020.12.002.
[24] Youn Cheol Park, Young Chul Kim, Man Ki Min, Performance analysis on a multi-type inverter air conditioner, Energ. Conver. Manage. 42 (13) (2001) 1607–1621, https://doi.org/10.1016/S0196-8904(00)00147-3.
[25] T.Q. Qureshi, S.A. Tassou, Variable-speed capacity control in refrigeration systems, Appl. Therm. Eng. 16 (2) (1996) 103–113.
[26] R.S. Adhikari, N. Aste, M. Manfren, D. Marini, Energy Savings through Variable Speed Compressor Heat Pump Systems, Energy Proc. 14 (2012) 1337–1342, https://doi.org/10.1016/j.egypro.2011.12.1098.
[27] Guilherme Z. Santos, Adriano F. Ronzoni, Christian J.L. Hermes, Performance characterization of small variable-capacity reciprocating compressors using a minimal dataset, Int. J. Refrig. 107 (2019) 191–201, https://doi.org/10.1016/j.ijrefrig.2019.07.014.
[28] Shuangquan Shao, Wenxing Shi, Xianting Li, Huajun Chen, Performance representation of variable-speed compressor for inverter air conditioners based on experimental data, Int. J. Refrig. 27 (8) (2004) 805–815, https://doi.org/10.1016/j.ijrefrig.2004.02.008.
[29] Ahri Standard Performance Rating of Modulating Positive Displacement Refrigerant Compressors, 2017.
[30] Hanlong Wan, Tao Cao, Yunho Hwang, Se-Dong Chang, Young-Jin Yoon, Machine-learning-based compressor models: A case study for variable refrigerant flow systems, Int. J. Refrig. 123 (2021) 23–33. 10.1016/j.ijrefrig.2020.12.003.
[31] Wan, Hanlong; Cao, Tao; Hwang, Yunho; Oh, Saikee. A review of recent advancements of variable refrigerant flow air-conditioning systems. Applied Thermal Engineering [online]. 2020. Vol. 169, no. October 2019, p. 114893. Doi. 10.1016/j.applthermaleng.2019.114893.
[32] Wheeler, Bob. *Cran - Package AlgDesign* [online]. v1.2.1. Available from: https://cran.r-project.org/web/packages/AlgDesign/index.html.
[33] Eric Winandy, O. Saavedra, Claudio Saavedra, Jean Lebrun, Experimental analysis and simplified modelling of a hermetic scroll refrigeration compressor, Appl. Therm. Eng. 22 (2) (2002) 107–120, https://doi.org/10.1016/S1359-4311(01)00083-7.
[34] *Toshiba Air Conditioning, Creator of modern Inverter Air Conditioning*. [online]. [Accessed 8 March 2023]. Available from: https://toshiba-aircon.com.au/toshiba-air-conditioning-creator-of-modern-air-conditioning/.
[35] *Bitzer Software*. [online]. [Accessed 6 May 2022]. Available from: https://www.bitzer.de/websoftware/Calculate.aspx?cid=1651820569375&mod=ESC.
[36] *Select Online*. [online]. [Accessed 9 September 2022]. Available from: https://selectonline.emersonclimate.eu/SelectOnline/main.
[37] *Coolselector*. [online]. [Accessed 17 May 2022]. Available from: https://coolselectoronline.danfoss.com/.
[38] *EN 13771. CEN*. 2016.